Int. J. Electrochem. Sci., 8 **(2013)** 6647 - 6655

International Journal of
ELECTROCHEMICAL
SCIENCE
www.electrochemsci.org

Structural, Thermal and Conductivity Studies of Magnesium Nitrate – Alumina Composite Solid Electrolytes Prepared via Sol-Gel Method

*Mazdida Sulaiman**, *A.A. Rahman and N.S. Mohamed*

Centre for Foundation Studies in Science, University of Malaya, 50603 Kuala Lumpur, Malaysia.
*E-mail: mazdidas@um.edu.my

Received: 6 March 2013 / *Accepted:* 13 April 2013 / *Published:* 1 May 2013

Composite solid electrolytes in the system $(1-x)Mg(NO_3)_2 - xAl_2O_3$ with $x = 0.0 - 0.5$ were synthesized by a sol-gel method. The synthesis was carried out at a low temperature with magnesium nitrate hexahydrate, as the starting material. The obtained magnesium composite dispersed with alumina were characterized by X-ray diffraction, differential scanning calorimetry, scanning electron microscopy, Fourier transform infrared spectroscopy and alternating current impedance spectroscopy. Structural analysis of the composite samples showed a transformation of the magnesium nitrate hexahydrate crystalline to amorphous magnesium nitrate and magnesium oxide. The composite sample with $x = 0.1$ and 0.2 exhibited high ionic conductivity of $\sim10^{-4}$ S cm^{-1} and $\sim10^{-6}$ S cm^{-1}, respectively, at room temperature due to the presence of MgO. This finding offers attractive future composite electrolytes for magnesium-based rechargeable batteries.

Keywords: Composite Material, Conductivity, Magnesium Nitrate, Alumina Composite

1. INTRODUCTION

Lithium ion conduction in composite solids has been an area under discussion for the past three decades since the discovery of high Li^+ ion conductivity at room temperature in $LiI - Al_2O_3$ system by Liang [1]. The rapid progress in portable consumer devices (such as iPads, iPhones and laptops), light vehicles, and hybrid electric vehicles has increased the need for novel and better energy sources. The lithium-based rechargeable batteries are the most worldwide consumed in terms of high energy density and low self discharge. Nevertheless, these battery systems have their limitations such as safety problems and high cost.

Recently, the development of magnesium rechargeable battery has drawn great attention of researches. This type of rechargeable battery is chosen since the magnesium is an active metal and can be used as anode material. Magnesium is cheaper and much safer to use than lithium. It is easier to handle magnesium than lithium because it is more stable in the air. There is an urgent need for research to develop this new rechargeable battery system. Moreover, its performance capabilities are expected to be very similar to those of lithium batteries [2,3].

Similar to the lithium rechargeable batteries, the electrolytes should have low vapor pressure, non-volatile and non-flammable properties. Lithium composite solid electrolytes were found to enhance not only the conductivity of the Li^+ ion conductor, but also its mechanical strength. Alternatively, suitable electrolyte system that is very safe and consistent is solid electrolyte conducting Mg^{2+} at ambient temperature. Solid electrolytes of magnesium salt – alumina composites offer attractive future composite electrolytes for magnesium-based rechargeable batteries.

In our previous work, we have successfully prepared composite solid electrolyte powder in the system $(1-x)LiNO_3 – xAl_2O_3$ using a sol-gel technique [4]. They were found to have high ionic conductivity values and could achieve 1.92×10^{-3} S cm^{-1} (for $x = 0.1$) at room temperature. In this work, composite solid electrolytes in the system $(1-x)Mg(NO_3)_2 – xAl_2O_3$, with $x = 0.0 – 0.5$ were prepared. The alumina powder was well dispersed into the magnesium nitrate salt via a sol-gel method.

The structure of the composite samples obtained were characterized using various methods such as X-ray diffraction (XRD), differential scanning calorimetry (DSC), scanning electron microscopy (SEM) and Fourier transform infrared spectroscopy (FTIR). The conductivity study was determined by alternating current (AC) impedance measurements.

The total ionic transport number (t_{ion}) of highest conducting sample was evaluated by Wagners's polarization method [5]. It is hoped that the magnesium composite solid electrolytes exhibit high ionic conductivity values and can be employed in the future magnesium rechargeable batteries.

2. EXPERIMENTAL

The magnesium nitrate hexahydrate $Mg(NO_3)_2.6H_2O$, alumina (Al_2O_3; particle size ~10 μm), citric acid and ethanol of high purity grade were obtained from Aldrich. The composite solid electrolyte samples are described by the general formula of $(1-x)Mg(NO_3)_2 – xAl_2O_3$ with $x = 0.1 – 0.5$ (mole). The samples were prepared via the sol-gel method. Both magnesium nitrate hexahydrate and alumina were weighed according to the mentioned general formula. For synthesizing the $(1-x)Mg(NO_3)_2 – xAl_2O_3$ composites, the starting host material of $Mg(NO_3)_2.6H_2O$ was first dissolved in deionized water that was mixed with ethanol, until a clear solution was obtained. The salt solution was then dispersed with the alumina powder by stirring it magnetically at ~40 °C on a hot plate for about 30 min, to get a homogeneous mixture. Subsequently, the mixture was added to a weighed citric acid and continuously stirred at a temperature range between 40 and 80 °C until a white gel was formed. The amount of the citric acid is equivalent to the mass of alumina. Finally, the gel was heated in an oven at 110 °C to slowly evaporate the solvents until dry. The composite sample obtained was then crushed in an agate mortar to a fine powder.

X-ray diffraction patterns of the composites were recorded using a D8 Advanced-Bruker X-ray diffractometer with Cu Kα radiation in the Bragg angle (2θ) range from 10 to 80°. The thermal stability of the composite sample was obtained on a METTLER TOLEDO DSC 822 with a continuous heating rate of 10 ^{o}C min^{-1}. The morphology of the samples was analyzed by scanning electron microscope (SEM) using an INCA Energy 200 instrument (Oxford Ins.). The FTIR spectra were recorded with a Perkin Elmer RX1 spectrometer.

The ionic conductivity measurements of the composite samples were carried out by impedance spectroscopy using a SOLATRON 1260 impedance analyzer over the frequency range of $10^{-1} – 10^{7}$ Hz. The conductivity measurements were conducted by sandwiching the composite pellet between two stainless steel electrodes for the temperature range from room temperature to 180 ^{o}C. The composite pellet was prepared by pressing composite powder under a pressure of 6 - 8 tones/cm^{2} at room temperature. The total ionic transport number (t_{ion}) was evaluated using Wagner's polarization method [5]. In this technique, the cell SS/ composite sample electrolyte /SS was polarized by applying a step potential of 500 mV. The resulting potentiostatic current was then monitored as a function of time. The value of t_{ion} was obtained using the following equation:

$$t_{ion} = \frac{i_T - i_e}{i_T} \qquad (1)$$

where i_T and i_e are total and residual current, repectively.

3. RESULTS AND DISCUSSION

Figure 1 shows the X-ray diffraction spectra of the prepared composite samples and pure $Mg(NO_3)_2.6H_2O$. The XRD pattern of the pure $Mg(NO_3)_2.6H_2O$ shows crystalline characteristic with predominant peaks at 2θ of 15^{o}, 27^{o}, 28^{o}, 30.3^{o} and 43.8^{o}. The rest of the peaks at 50.7^{o}, 56^{o} and 60.6^{o} show that there are traces amount of magnesium nitrate hydrate of $Mg(NO_3)_2.2(H_2O)$. These minor peaks are not found in all composite samples with $x = 0.1 – 0.5$. However, additional peaks observed in between 15^{o} to 27^{o} at $x = 0.1$ and 0.2 may be attributed to the $Mg(NO_3)_2.2(H_2O)$ peaks due to incomplete dehydration of $Mg(NO_3)_2.6H_2O$. The diffractogram of the composite samples shows the characteristic peaks of Al_2O_3 at 2θ of 25.6^{o}, 35.2^{o}, 37.7^{o}, 43.6^{o}, 52.5^{o}, 57.5^{o}, 61.6^{o}, 66.5^{o}, 68.2^{o} and 76.8^{o} along with some $Mg(NO_3)_2.6H_2O$ peaks. This confirms the composite nature of the samples with $x = 0.1 – 0.5$. The disappearance of the $Mg(NO_3)_2.6H_2O$ peaks indicates transformation of $Mg(NO_3)_2.6H_2O$ to $Mg(NO_3)_2$ and MgO in all composite samples.

The $Mg(NO_3)_2.6H_2O$ peaks with low intensity appeared at 15^{o}, 27^{o}, 28^{o}, 30.3^{o} for composite sample with $x = 0.1 – 0.3$. These peaks are attributed to the solid-state phase transition which is discussed in the following section. The XRD pattern also indicates that the $Mg(NO_3)_2$ exists as an amorphous phase in the composite sample with $x = 0.4$, as only crystalline Al_2O_3 peaks can be identified. The X-ray diffraction study for the prepared composites in the system $(1-x)Mg(NO_3)_2 – xAl_2O_3$ show formation of magnesium oxide (MgO) compound at $x = 0.1$ and 0.2, with a very poor crystallinity as can be seen in Figure 1. The broad diffraction peaks of MgO can be detected at 2θ of 38.2^o and 43.4^o [3,6,7]. Bokhimi *et al* [7] reported that at this low temperature, the phase of MgO is amorphous.

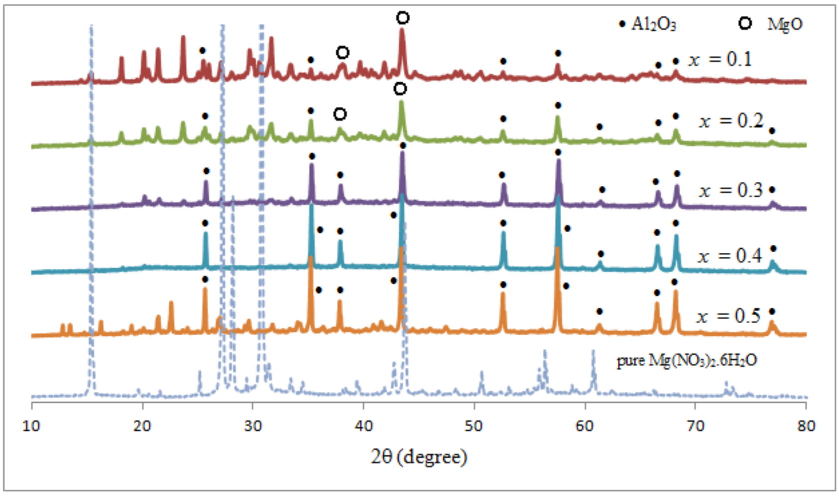

Figure 1. XRD patterns of (1-x) $Mg(NO_3)_2 - xAl_2O_3$ composites.

The DSC curves of pure Mg $(NO_3)_2.6H_2O$ and the prepared composite samples are shown in Figure 2(a). Two endothermic peaks are identified in the curve for the pure $Mg(NO_3)_2.6H_2O$ compound. The two endothermic peaks at 74 °C and 90 °C, correspond to solid state phase transition and melting (T_m) of the compound, respectively [8,9]. There is no endothermic peak indicating the melting of $Mg(NO_3)_2.6H_2O$ in the curve of the composite with $x = 0.1 – 0.5$. The absence of the peak means that the crystalline $Mg(NO_3)_2.6H_2O$ has undergone a transition phase during the preparation process. The possible transformation of the crystalline could be as follow [7]:

$$Mg(NO_3)_2.6H_2O_{(s)} \xrightarrow{\text{dissolution}} Mg(NO_3)_{2\,(s)} + 6H_2O_{(g)} \qquad (2)$$

$$2Mg(NO_3)_{2\,(s)} \longrightarrow 2MgO_{(s)} + 4NO_{2(g)} + O_{2(g)} \qquad (3)$$

Incongruent melting of the solid state phase transition is observed between ~50 °C and ~80 °C for the curves of the composite samples with $x = 0.1 – 0.5$ (except at $x = 0.4$). The polymorphic changes occurred due to the interaction with the alumina particles in the composites. The formation of MgO in composite samples with $x = 0.1$ and $x = 0.2$ are obvious and this could be due to the limited amount of alumina particles present in the composites so that no blocking effect occurred for the transformation of phases of the crystalline. However the solid-state of $Mg(NO_3)_2$ exists as an amorphous phase in the composite sample with $x = 0.4$, as no incongruent temperature of melting is detected. The presence of the phase is confirmed by the XRD analysis discussed earlier. Figure 2(b) shows a small endothermic peak around 390 °C for the MgO formed at $x = 0.1$ and 0.2 [10].

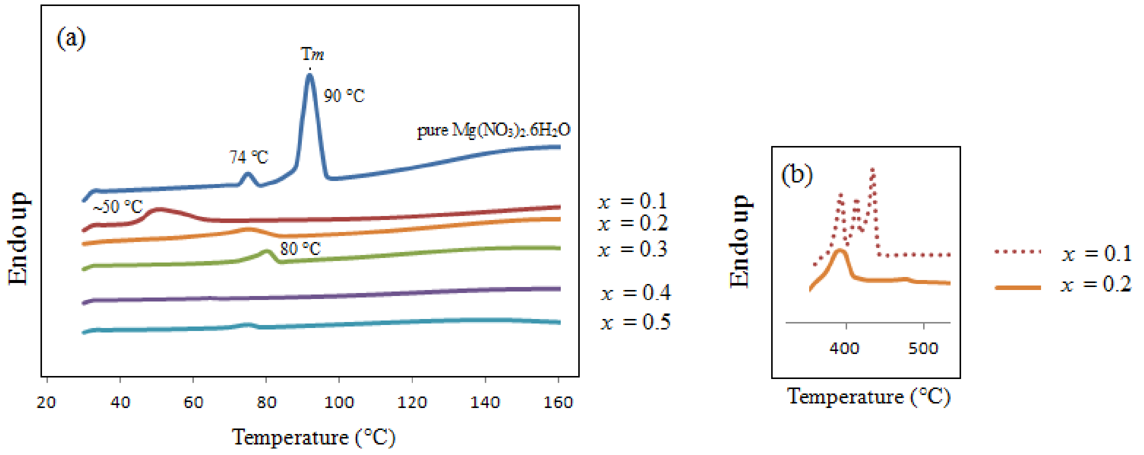

Figure 2. DSC curves for **(a)** pure $Mg(NO_3)_2.6H_2O$ and $(1-x)Mg(NO_3)_2 - xAl_2O_3$ composites. **(b)** Formation of MgO at $x = 0.1 - 0.2$.

The FTIR spectra of $Mg(NO_3)_2.6H_2O$ and the composite samples with $x = 0.1 - 0.5$ in the wavenumber range 1600-600 cm^{-1} are presented in Figure 3. The spectrum of the $Mg(NO_3)_2.6H_2O$ shows a strong absorption band at 1347 cm^{-1} and two medium bands at 818 and 730 cm^{-1}. Those bands are ascribed to the asymmetric stretching (ν_3), out-of-plane deformation (ν_2) and in-plane deformation (ν_4) modes of NO_3^- ion, respectively [11,12,13]. These characteristic bands of the nitrate group are also observed in all of the composite samples ($x = 0.1 - 0.5$) in Figure 3. Therefore, we can conclude that the $Mg(NO_3)_2$ phase is present in the composite samples with $x = 0.1 - 0.5$. The symmetry stretch mode (ν_1) of NO_3^- for pure $Mg(NO_3)_2.6H_2O$ is observed as a very weak band at 1058 cm^{-1}. Addition of alumina, Al_2O_3 caused ν_1 mode to shift toward higher wavenumber of ~1068 cm^{-1} accompanied by an increase in the half-band width which can be ascribed to the presence of an amorphous phase [14]. The ν_1 mode shift can clearly be observed in the composite sample with $x = 0.1 - 0.3$. However, the addition of alumina leads to the splitting of the ν_1 band at $x = 0.4$ and 0.5. These phenomena show the mixture characteristic of the composite samples with $x = 0.1 - 0.5$.

The composite samples with $x = 0.2 - 0.5$ show two peaks with maxima at ~1429 and ~1318 cm^{-1}, resulting from the splitting of the ν_3 mode of surface nitrate. There is no ν_3 mode splitting occurs at $x = 0.1$. The appearance of the two peaks is indicative of monodentate orientation of nitrate ions [15]. From the literature, the bands observed at ~751, ~816 and ~1068 cm^{-1} suggest the bidentate type of NO_3^- ion upon contacting with Mg^{2+} [15]. As observed at $x = 0.1 - 0.5$, the frequency of ν_4 shifts from 730 to ~752 cm^{-1} and the ν_2 shifts from 819 to ~816 cm^{-1}. The monodentate and bidentate types of nitrate ion revealed the formation of Mg^{2+} and NO_3^- ion pairs in the composite samples with $x = 0.1 - 0.5$. It appears that the nitrate ion contacting Mg^{2+} in monodentate type converts to bidentate type as the alumina content increases. The contact ion pairs do affect the conductivity behavior of the composites. The explanation is discussed in the following section.

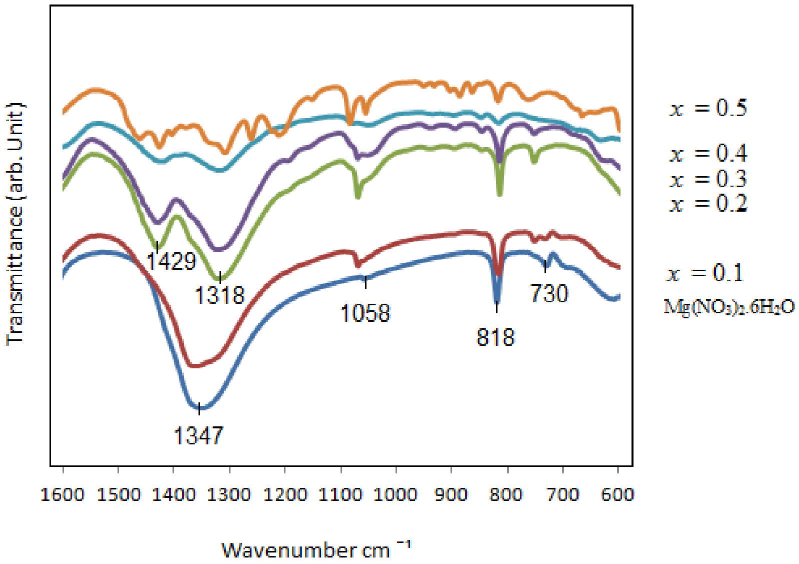

Figure 3. FTIR of $Mg(NO_3)_2.6H_2O$ and $(1\text{-}x)Mg(NO_3)_2 - xAl_2O_3$ composites.

Figure 4 shows the cross-sectional morphology of the composite sample with $x = 0.4$. Figure 4(a) indicates the appearance of crystalline (region A) and amorphous (region B) features in the composite sample. The crystalline and amorphous regions are attributed to the Al_2O_3 and $Mg(NO_3)_2$, respectively as discussed earlier in the XRD and DSC sections. Figure 4(b) depicts that the composite sample is dominated by the crystalline phase of $Mg(NO_3)_2$ and this feature could impede the conductivity behavior.

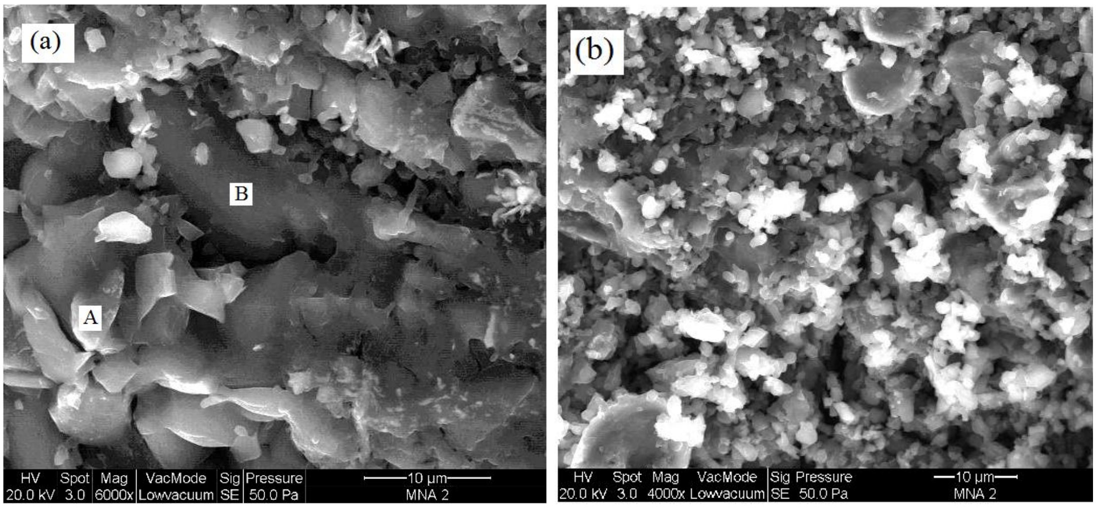

Figure 4. Cross-section morphology of composite sample with $x = 0.4$ magnified at **(a)** 6000X and **(b)** 4000X.

The temperature dependency of conductivities for $(1\text{-}x)Mg(NO_3)_2 - xAl_2O_3$ composites prepared is shown in Figure 5. In general, at $x = 0.1 - 0.5$, the conductivity increases with increase in temperature. Two conductivity changes occur in the system at temperature around 70 °C and 120 °C.

The low conductivity values below the temperature region of 70 °C at $x = 0.3 – 0.5$ reflect greater association of Mg^{2+} with NO_3^- in the composites as confirmed by the FTIR analysis discussed earlier. The strong electrostatic forces caused immobility of the Mg^{2+} ion in the composites.

However, the presence of MgO amorphous phase in the composite samples with $x = 0.1$ and 0.2 results in an increase in conductivity to the order of $\sim 4.0 \times 10^{-4}$ S cm^{-1} and $\sim 4.0 \times 10^{-6}$ S cm^{-1}, respectively, at room temperature. In this case, the high ionic conductivity reflects the dissociation of Mg^{2+} and NO_3^- ion pairs into free ions with the appearance of MgO [3].

The MgO particles are slightly electronegative in nature and hence, incorporate with the Mg^{2+} ions to form MgO: Mg^{2+} species. The formation of the species occurs at the interface regions between MgO and the ionic salt. The reaction of the formation of MgO: Mg^{2+} species is reversible and is as follows:

$$MgO + Mg^{2+} \rightleftharpoons MgO\text{: }Mg^{2+} \qquad (4)$$

This new region, namely space-charge region induces a local electric field and is responsible for the enhanced Mg^{2+} ion mobility in the composite sample with $x = 0.1$. Similar observation has been reported in the literature [16]. The value of the ionic transport number is 0.85 for composite sample with $x = 0.1$. This suggests that the composite sample is predominantly an ionic conductor. It has been observed that the solid composite electrolyte in the system $(1-x)Mg(NO_3) – xAl_2O_3$ with $x = 0.1$, exhibits ionic conductivity at room temperature that is quite similar to electrolyte of $(1-x)LiNO_3 – xAl_2O_3$ [4]. The conductivity of the magnesium composite electrolyte is even higher than the composites based on lithium salts reported in the literature [1,17,18]. In this case, it is possible to switch Li^+ ions with Mg^{2+} ions as the charge carrier for new rechargeable battery system.

As observed, the conductivity at $x = 0.2$ is lower than $x = 0.1$. The decrease is related to the bidentate type of NO_3^- ion in the composite sample with $x = 0.2$ which leads to less number of free Mg^{2+} ion. The conductivity phenomenon around 70 °C shows a change of phase is in progress in all the composite samples with $x = 0.1 – 0.5$. This is attributed to the incongruent melting of the solid-state phase transition as mentioned earlier in the DSC analysis.

Starting from the temperature of 120 °C, the conductivity continues to increase to the order of $\sim 10^{-4}$ to 10^{-3} S cm^{-1}. The increase in temperature results to the ion dissociation in the $Mg(NO_3)_2$ phase. Thus, the Mg^{2+} ion mobility increases especially after complete melting of magnesium nitrate beyond this temperature [19].

The experiment results confirm that the formation of MgO and at the same time the presence of free Mg^{2+} ion contribute greatly to the enhancement of conductivity in the $MgNO_3 – Al_2O_3$ composite system. Such behavior has also been observed for a magnesium ion-conducting gel polymer electrolyte [3]. In order to get better conductivities and to be better magnesium rechargeable batteries, an additional of MgO particles could be dispersed into the $MgNO_3 – Al_2O_3$ composite system.

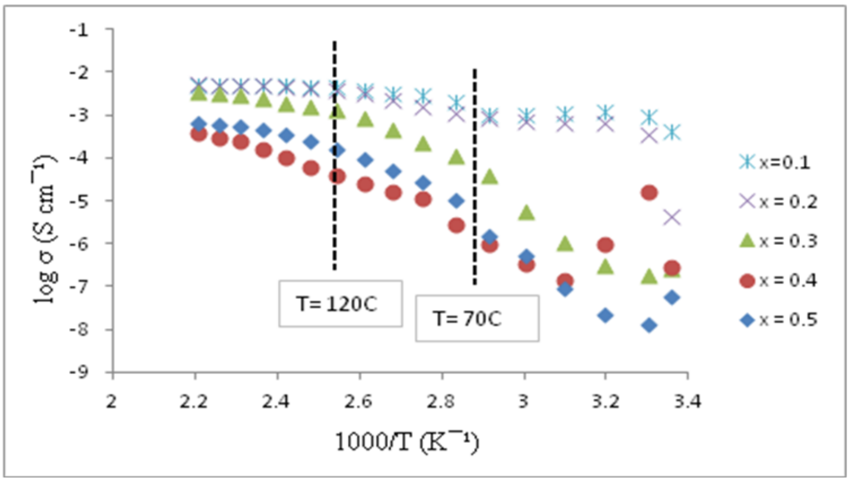

Figure 5. Temperature dependency of conductivities for (1-x)$Mg(NO_3)_2$-$x Al_2O_3$ composites.

4. CONCLUSION

Magnesium composites in the system (1-x)$Mg(NO_3)_2$ – $x Al_2O_3$ had been successfully synthesized via a sol-gel method at low temperature. We had studied the structural and conductivity behavior of the obtained magnesium composites with compositions from x = 0.1 to 0.5. The peaks from the XRD spectrum indicate possible transformation of $Mg(NO_3)_2.6H_2O$ to $Mg(NO_3)_2$ and MgO. The appearance of MgO can be seen in the composite samples with x = 0.1 - 0.2 and further confirmed by the DSC and conductivity results. The thermal analysis showed an incongruent melting of the solid state phase transition that occurred between ~50 °C and ~80 °C in the composite samples with x = 0.1 – 0.5 (except at x = 0.4). This polymorphic change occurred due to the interaction with the alumina powder in the composites. The prepared composites have low conductivity below the temperature region of 70 °C due to the strong association between Mg^{2+} and NO_3^- ion pairs. The FTIR results revealed the monodentate and bidentate types of nitrate ion in the composite samples thus, the formation of Mg^{2+} and NO_3^- ion pairs contact. However, the composite samples with x = 0.1 and x = 0.2 exhibited high ionic conductivity at room temperature in the order of ~4.0×10^{-4} S cm^{-1} and ~4.0×10^{-6} S cm^{-1}, respectively due to the presence of MgO amorphous phase. Thus, the magnesium composite solid electrolyte in the system (1-x)$Mg(NO_3)_2$ – $x Al_2O_3$ can be considered as a new class of magnesium based composite electrolyte and could be employed in the magnesium rechargeable batteries.

ACKNOWLEDGMENT
The authors are pleased to acknowledge the financial support from University of Malaya (Grant No.RG021/09AFR), for this research project.

References

1. C. C. Liang, *J. Electrochem. Soc.*, 120 (1973) 1289.

2. D. Aurbach, Y. Gofer, Z. Lu, A. Schechter, O. Chusid, H. Gizbar, Y. Cohen, V. Ashkenazi, M. Moshkovich, R. Turgeman and E. Levi, *J. Power Sources*, 97 (2001) 28.
3. G. P. Pandey, R. C. Agrawal and S. A. Hashmi, *J. Power Sources*, 190 (2009) 563.
4. M. Sulaiman, N. A. Dzulkarnain, A. A. Rahman and N. S. Mohamed, S. *Solid State Sci.*,14 (2012) 127.
5. S. Chandra, *Superionic solids: Principle and applications;* North – Holland (1981).
6. S. Veldurthi, C. –H. Shin, O. –S. Joo and K. –D. Jung, *Micropor Mesopor Mat*., 152 (2012) 31.
7. Bokhimi, A. Morales, T. Lopez and R. Gomez, *J. Solid State Chem.*, 115 (1995) 411.
8. J. Schaefer and M. Grube, *Mater Res Bull.*, 30 (1995) 1235.
9. S. Cantor, *Thermochim Acta*, 33 (1979) 69.
10. C. N. R. Rao, and K. S. Pitzer, *J. Phys Chem.*, 64 (1960) 282.
11. A. Wahab and S. Mahiuddin, *J. Chem Eng Data*, 54 (2009) 436.
12. A. Wahab, S. Mahiuddin, G. Hefter, W. Kunz, B. Minofar and P. Jungwirth, *J. Phys Chem. B*, 109 (2005) 24108.
13. A. B. Béléké, M. Mizuhata, A. Kajinami and S. Deki, *J. Colloid Interf Sci.*, 268 (2003) 413.
14. N. F. Uvarov, P. Vanek, Y. I. Yuzyuk, V. Zelezny, V. Studnicka, B. B. Bokhonov, V. E. Dulepov and J. Petzelt, *Solid State Ionics*, 90 (1996) 201.
15. T. G. Chang and D. E. Irish, *J. Phys Chem.*, 77 (1973) 52.
16. G. P. Pandey, R. C. Agrawal, and S. A. Hashmi, *J. Phys Chem. Solids*, 72 (2011) 1408.
17. M. P. Vinod and D. Bahnemann, *J. Solid State Electrochem.*, 6 (2002) 498.
18. L. Chen, Z. Zhao, C. Wang and Z. Li, *Acta Phys Sin.*, 34 (1985) 1027.
19. K. Nagano, K. Ogawa, T. Mochida, K. Hayashi and H. Ogoshi, *Appl Therm Eng.*, 24 (2004) 209.